

Figure 1: SCOPE SHM platform

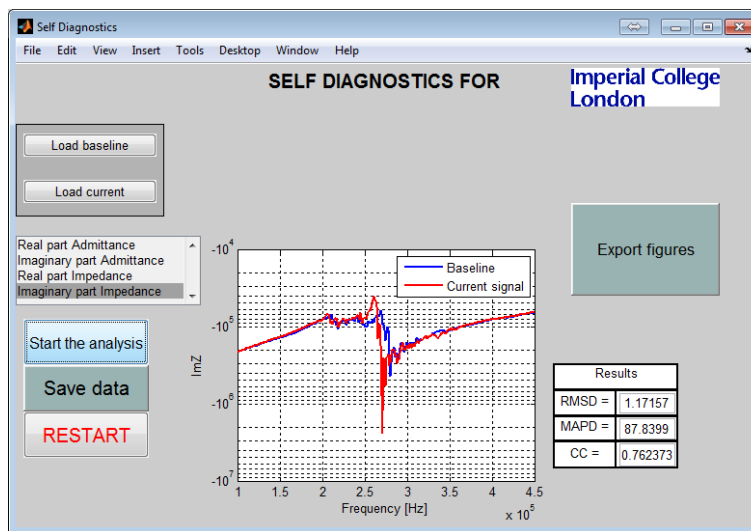
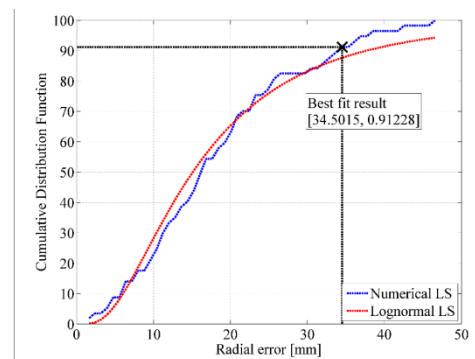
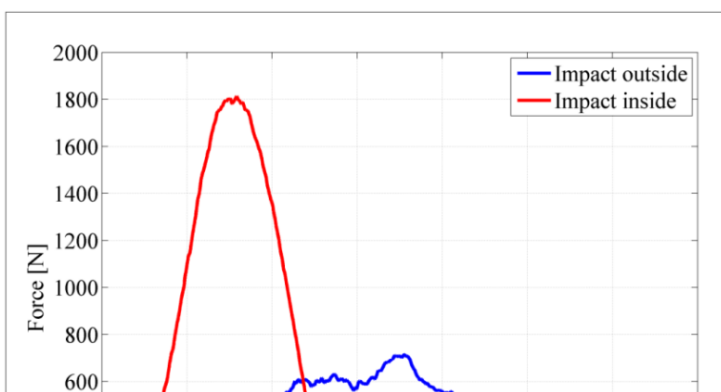
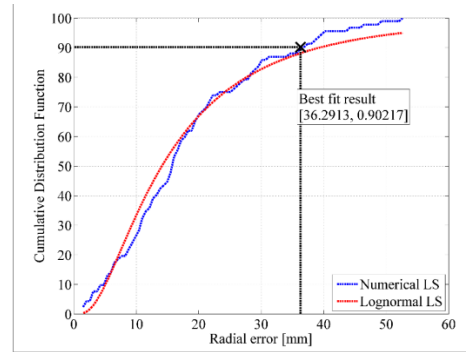


Figure 2: Self-diagnostic module - SCOPE platform



(b) POD for impact location, outer panel

(a) Contact force



(c) POD for impact location, inner panel

Figure 3: Examples of impact force caused from impacts on inside and outside of the panel

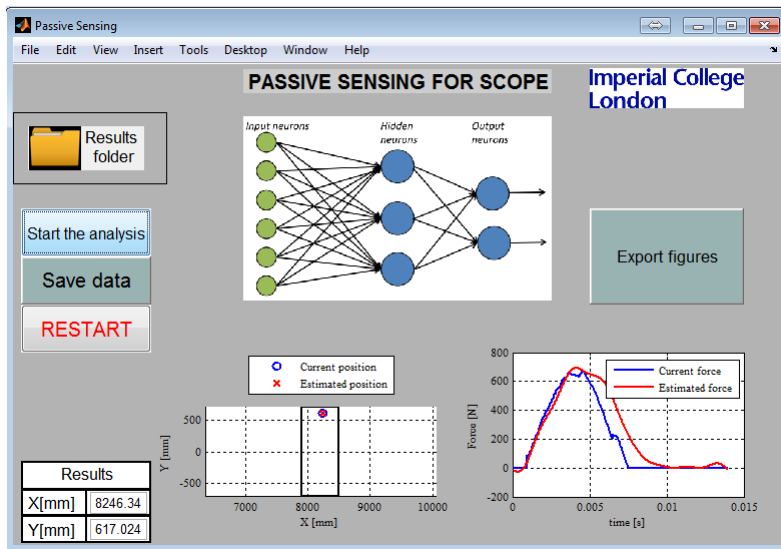


Figure 4: Passive sensing module - SCOPE platform

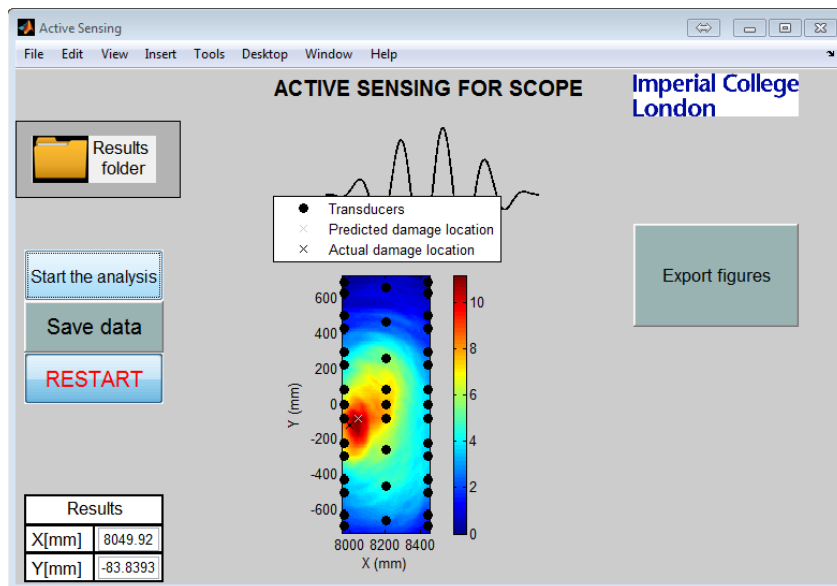


Figure 5: Active sensing module - SCOPE platform

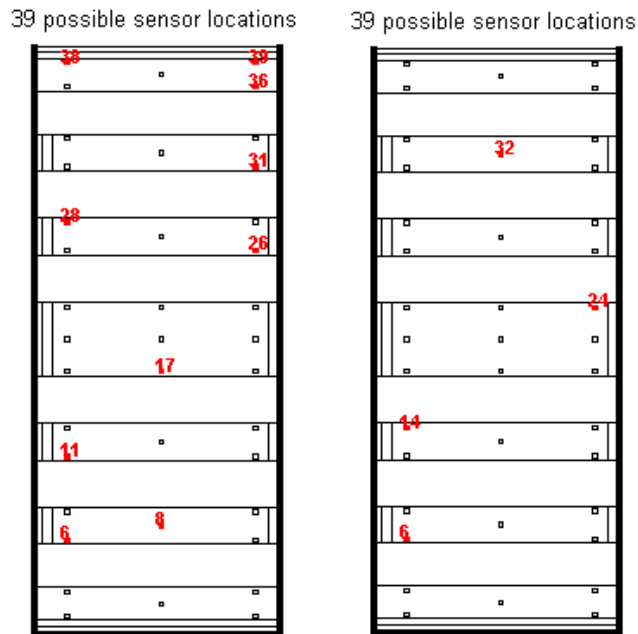
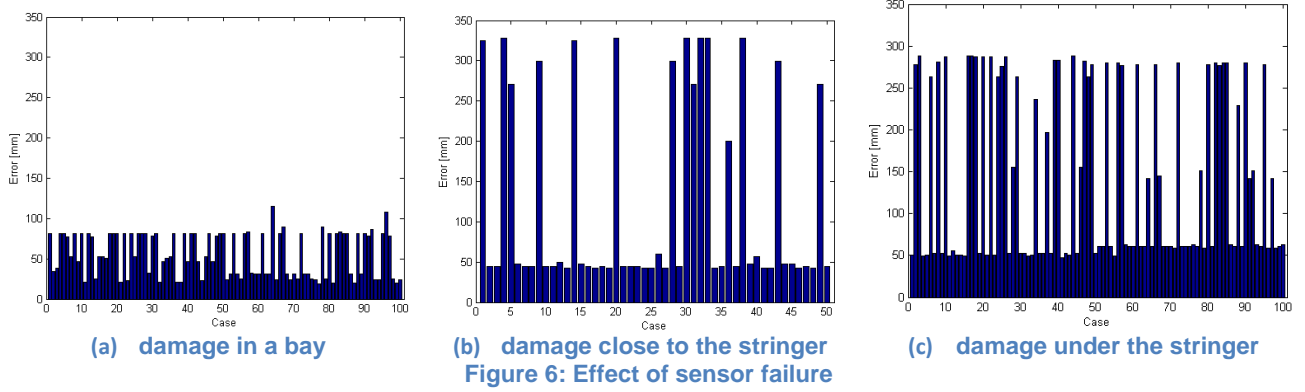
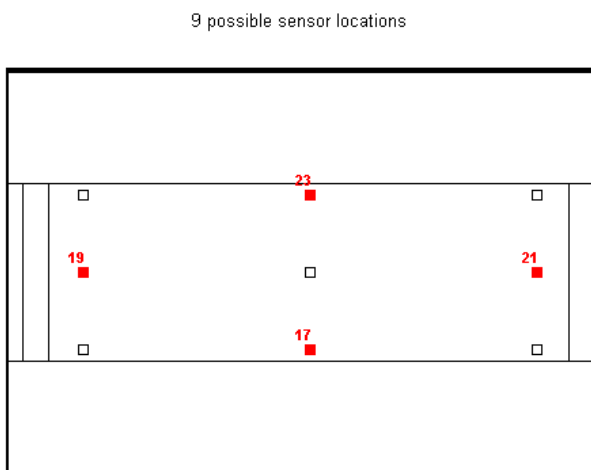
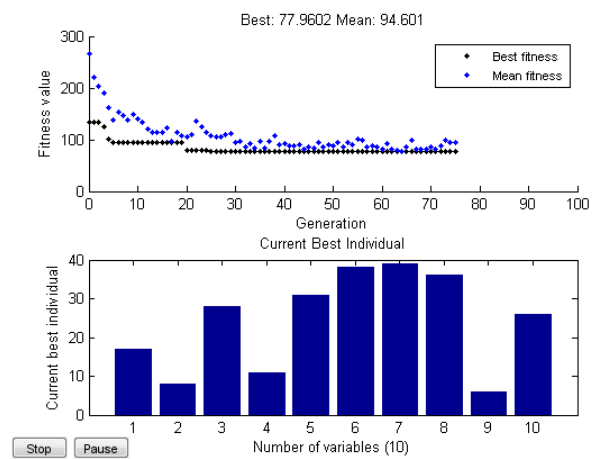


Figure 7: Best sensor positions for an investigation using 8 and 4 sensors in seven bays.

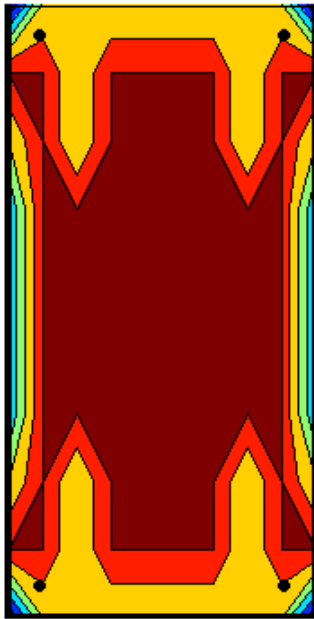


(a) Best 4 sensors placement in the central bay

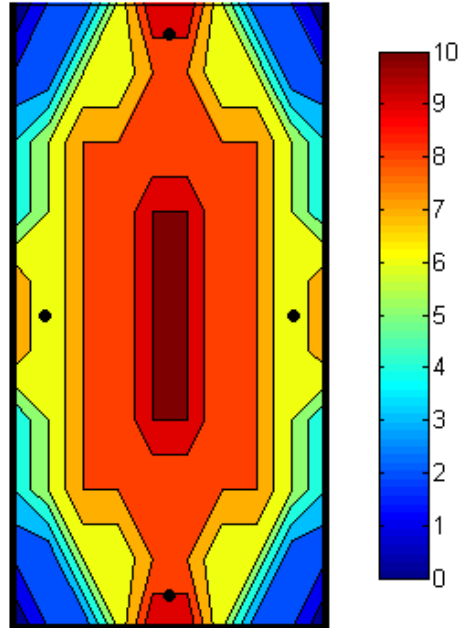


(b) Example of GA results

Figure 8: Example of GA results.

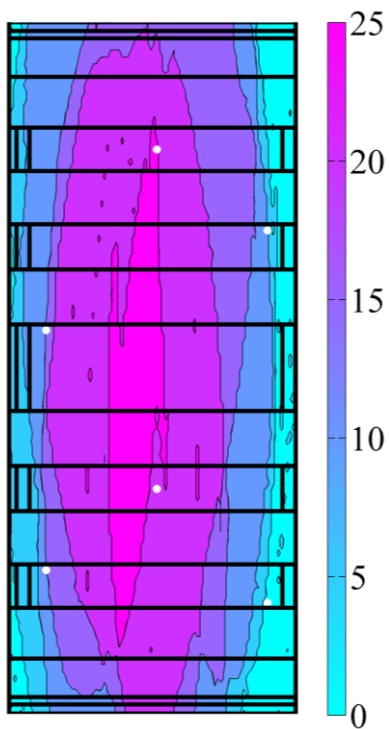


4 sensors at the corners.



4 sensors at mid-edge position

Figure 9: Example of coverage area related to different transducer location



39 possible sensor locations

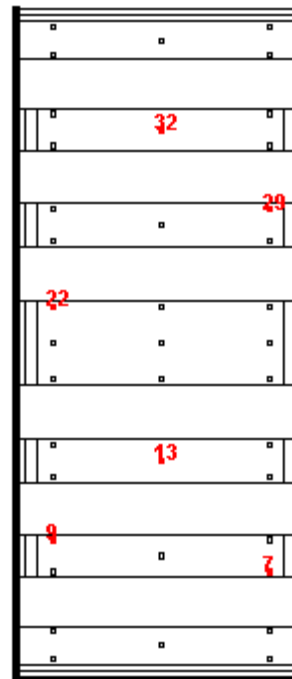


Figure 10: Coverage and positioning for 6 sensors

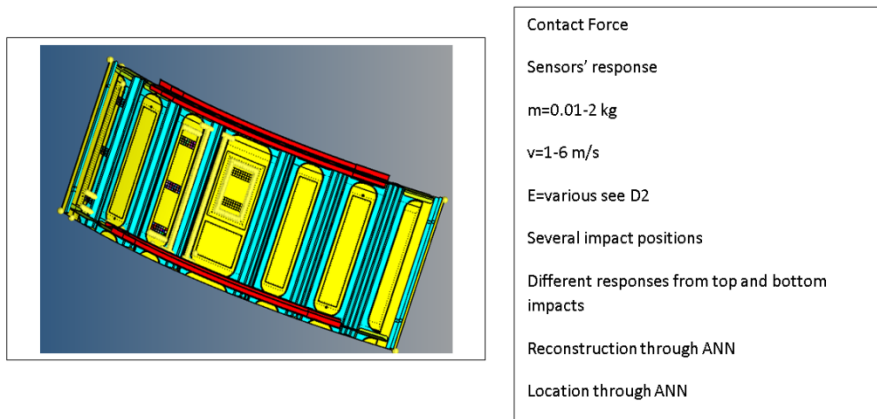
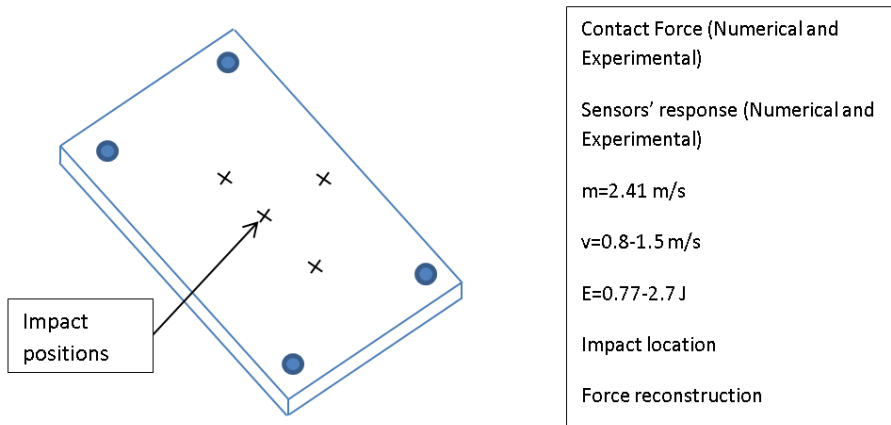
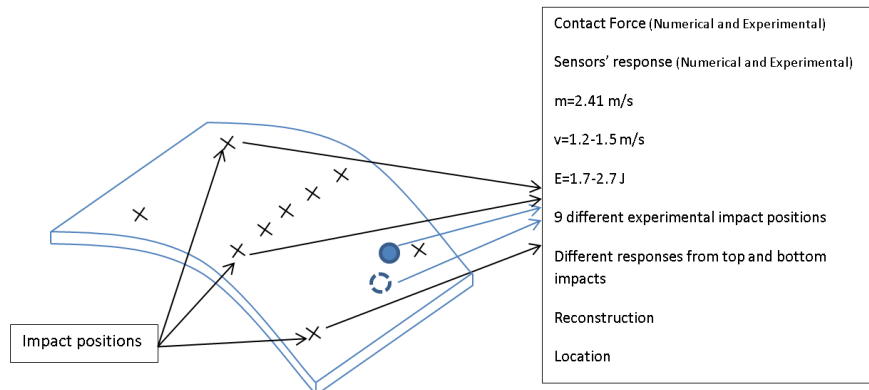


Figure 11: Building block approach for validation of passive sensing.

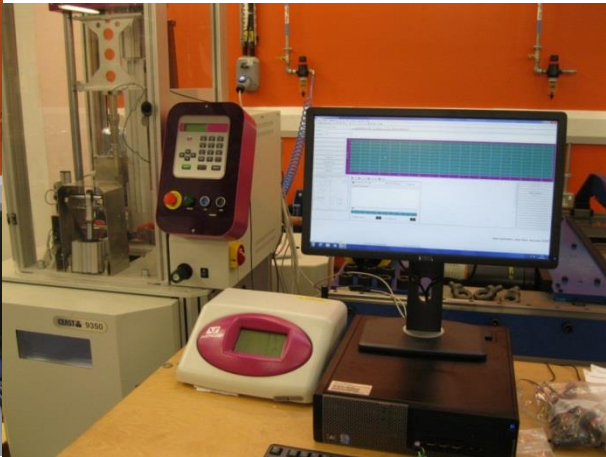


Figure 12: Drop tower used for the validation of passive sensing.

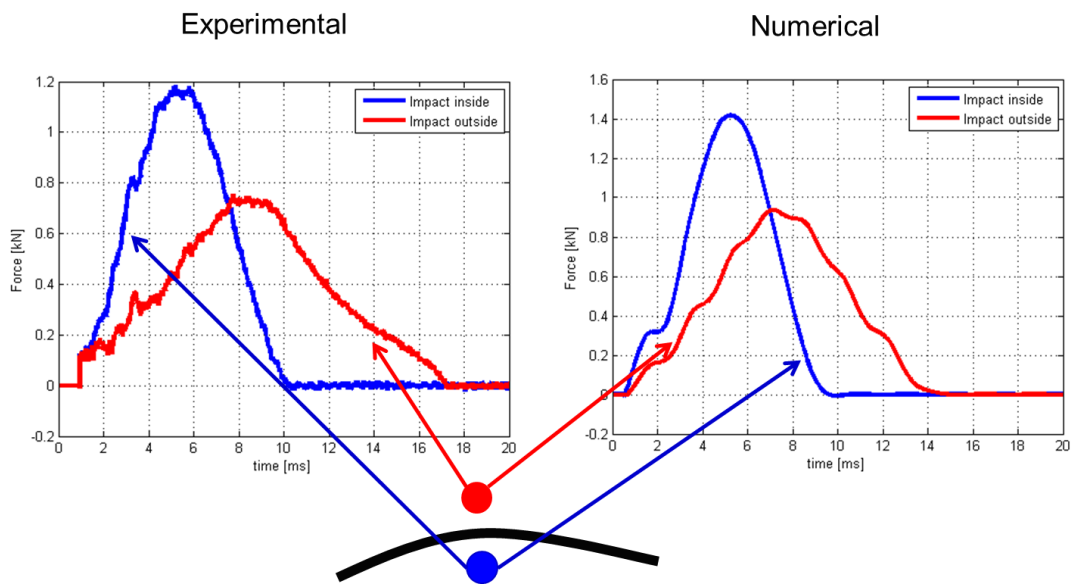


Figure 13: Validation of contact force.

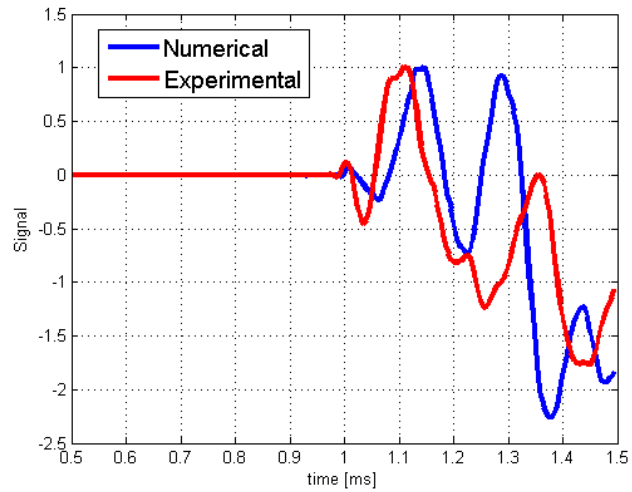


Figure 14: Validation of the PZT signal.

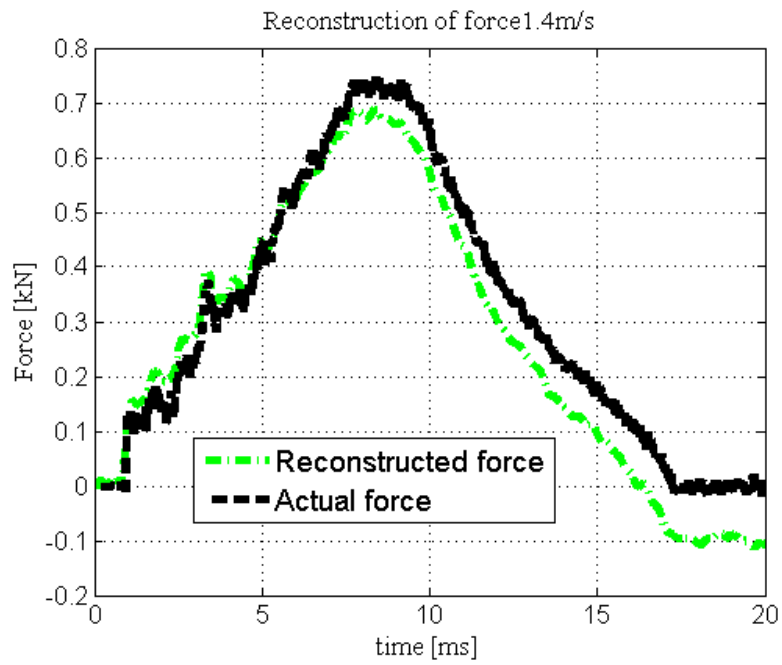


Figure 15: Experimental force reconstruction.

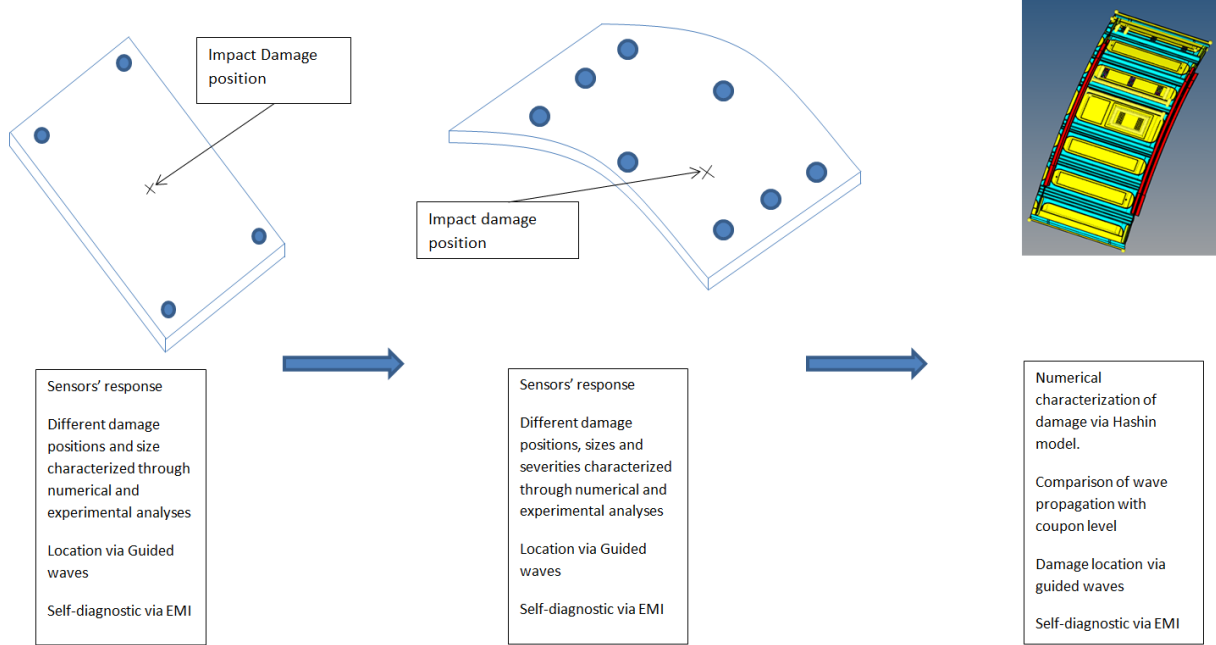


Figure 16: Validation approach for active sensing.

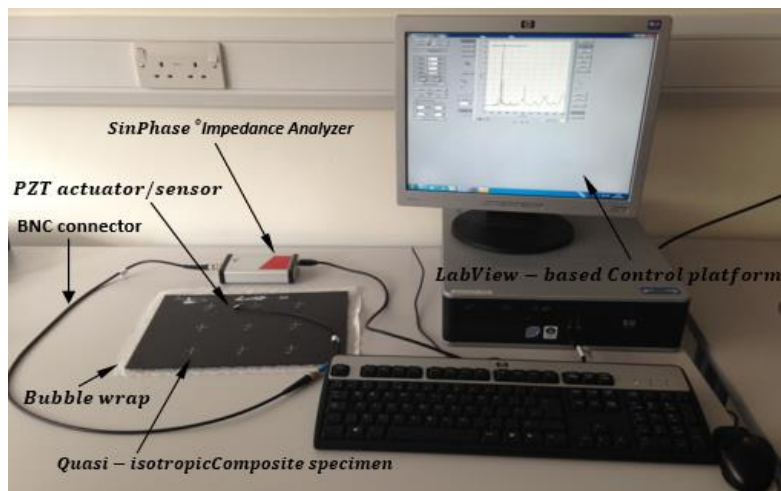
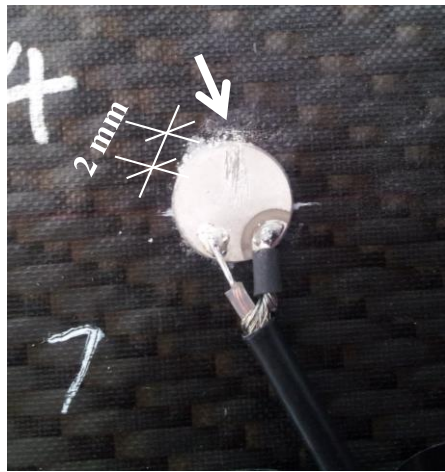


Figure 17: Experimental setup for the EMI investigation.





(a) Crack 1



(b) Crack 2

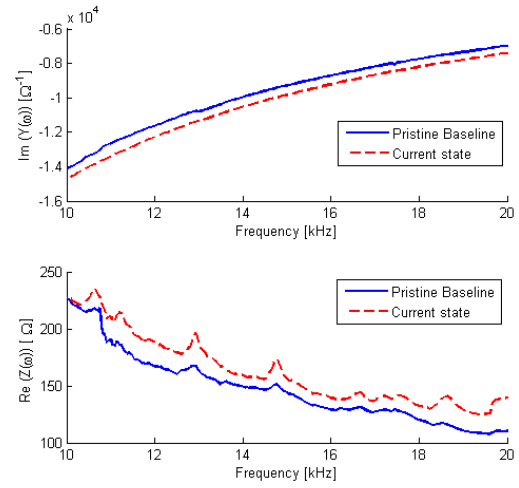
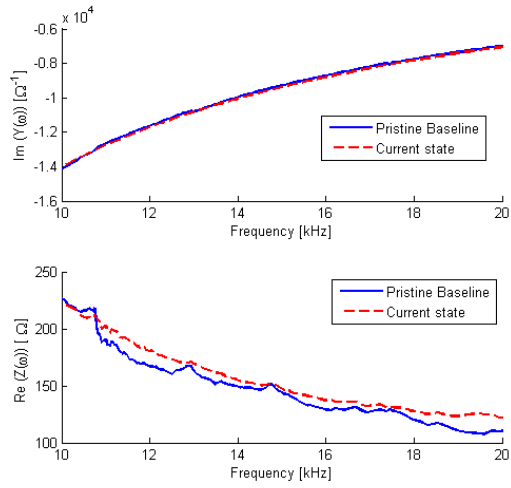
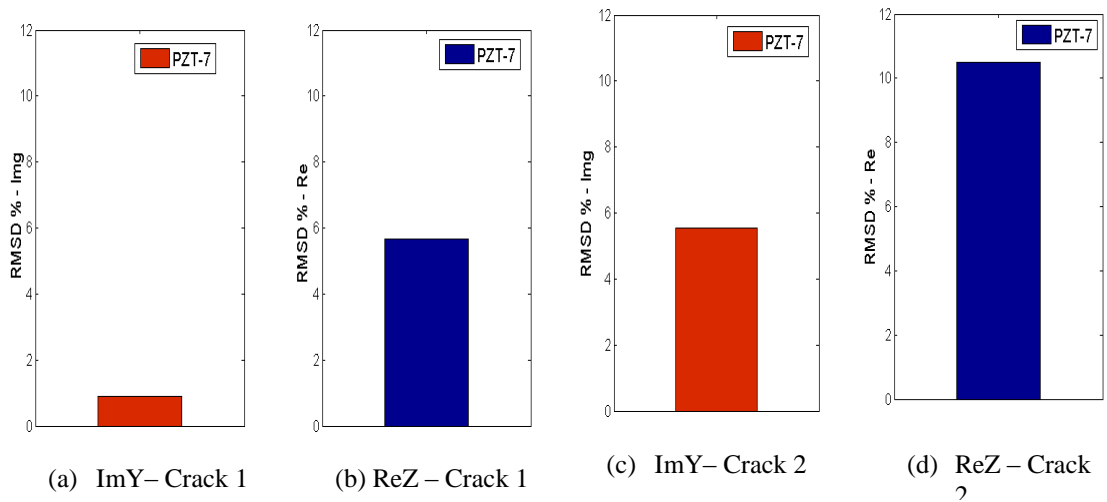


Figure 18: Self-diagnostics via EMI for a cracked PZT.



(a) ImY - Crack 1

(b) ReZ - Crack 1

(c) ImY - Crack 2

(d) ReZ - Crack 2

Figure 19: Crack evaluation via RMSD.

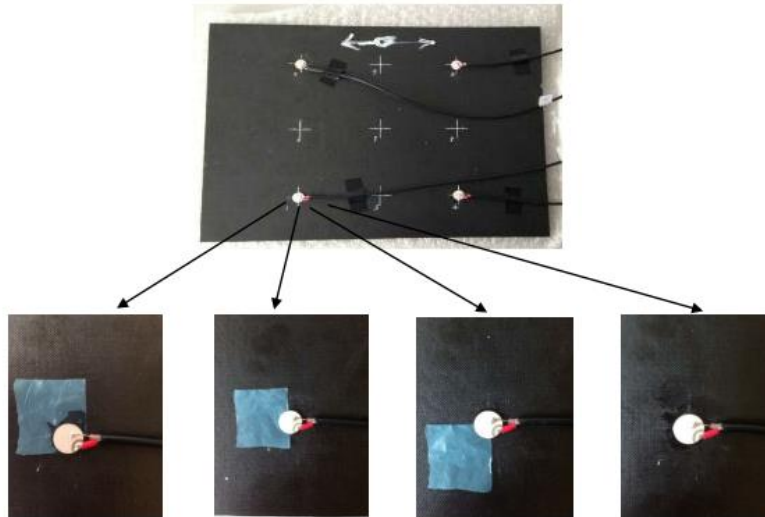


Figure 20: Different debonding cases.

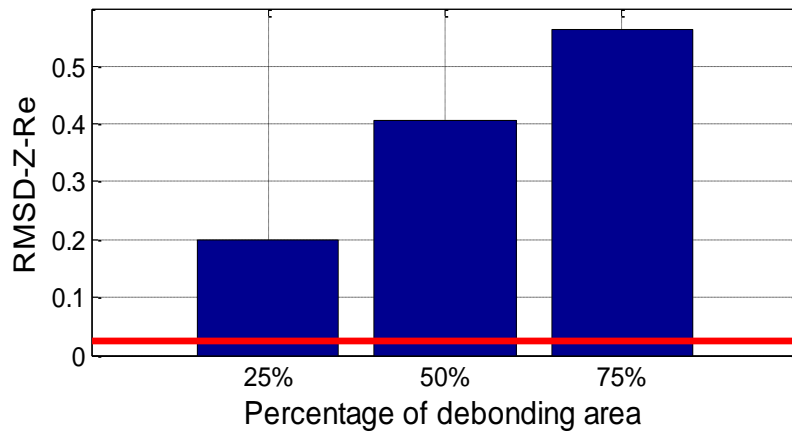


Figure 21: Debonding evaluation via EMI.

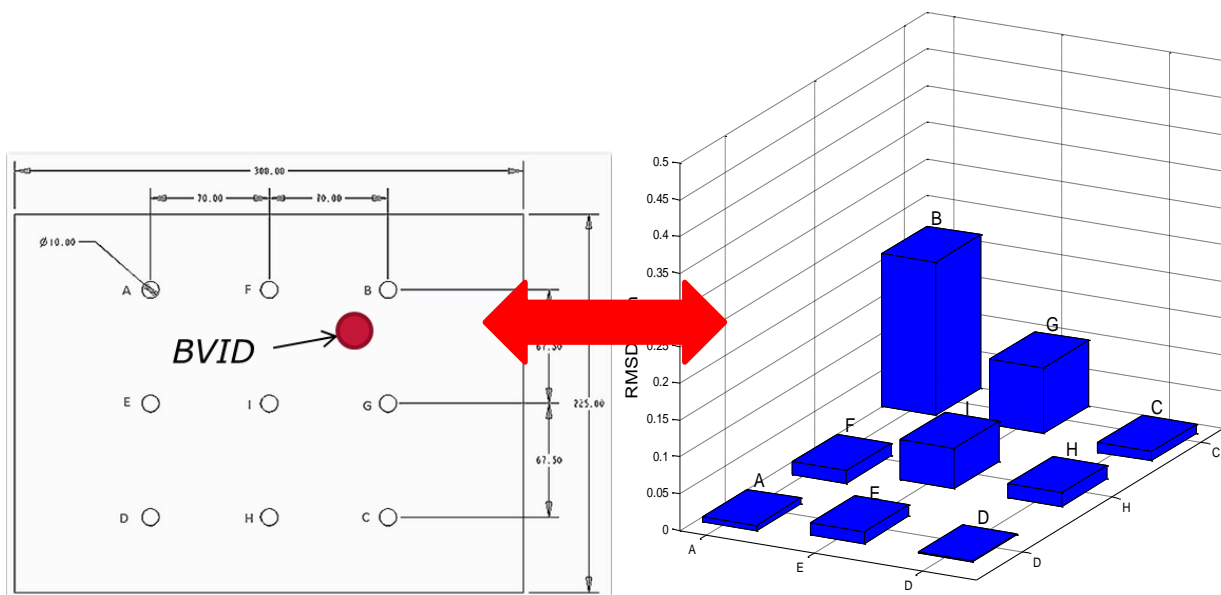


Figure 22: Damage evaluation at coupon level via EMI.

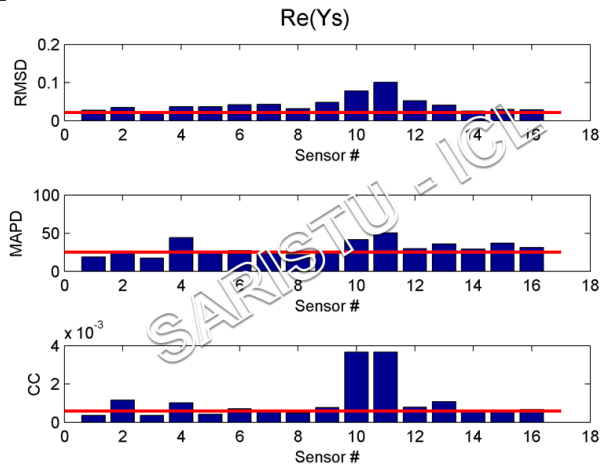
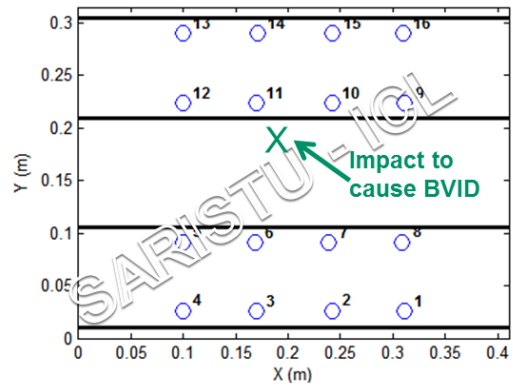


Figure 23: Damage detection via EMI at sub-component level [14].

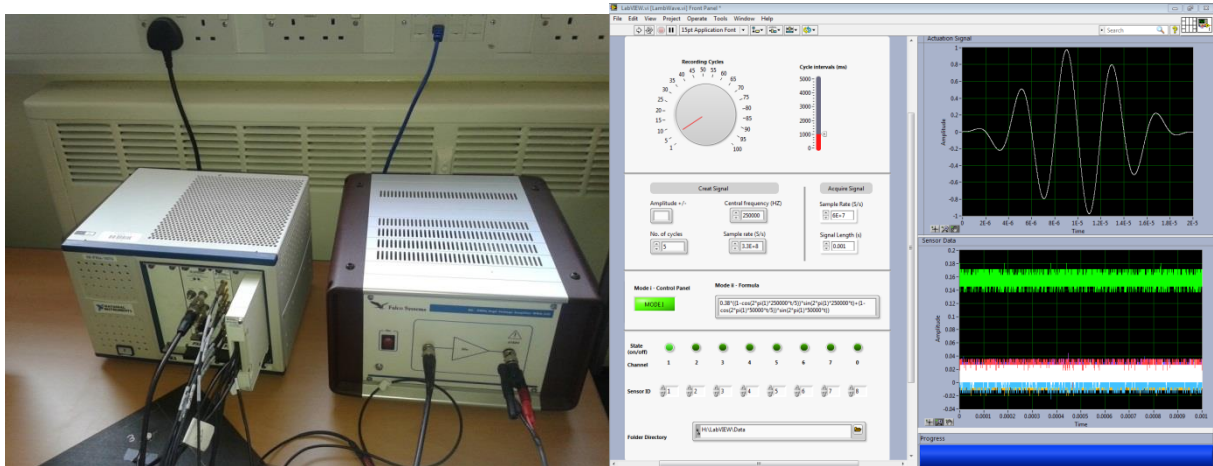


Figure 24: Experimental setup for Lamb wave investigations.

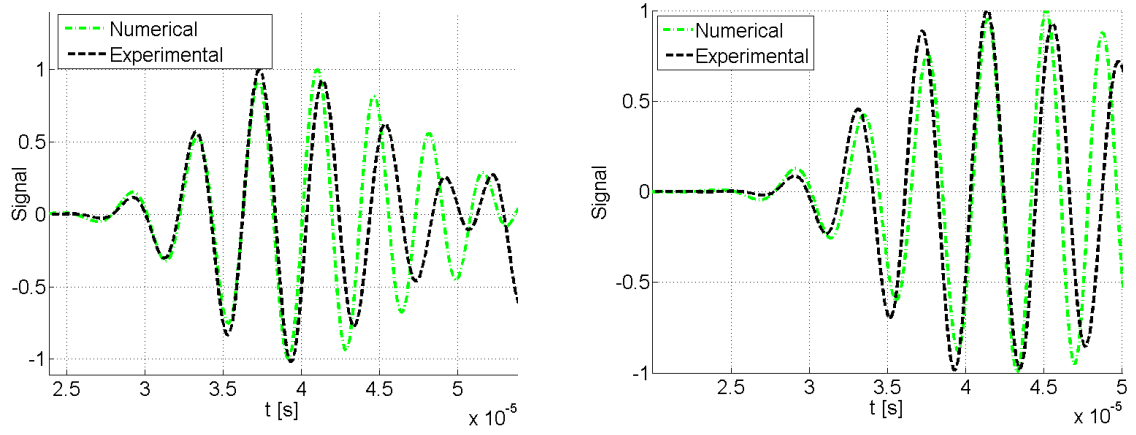


Figure 25: Validation of Lamb-wave signals.



Figure 26: Curved coupon panel under analysis.

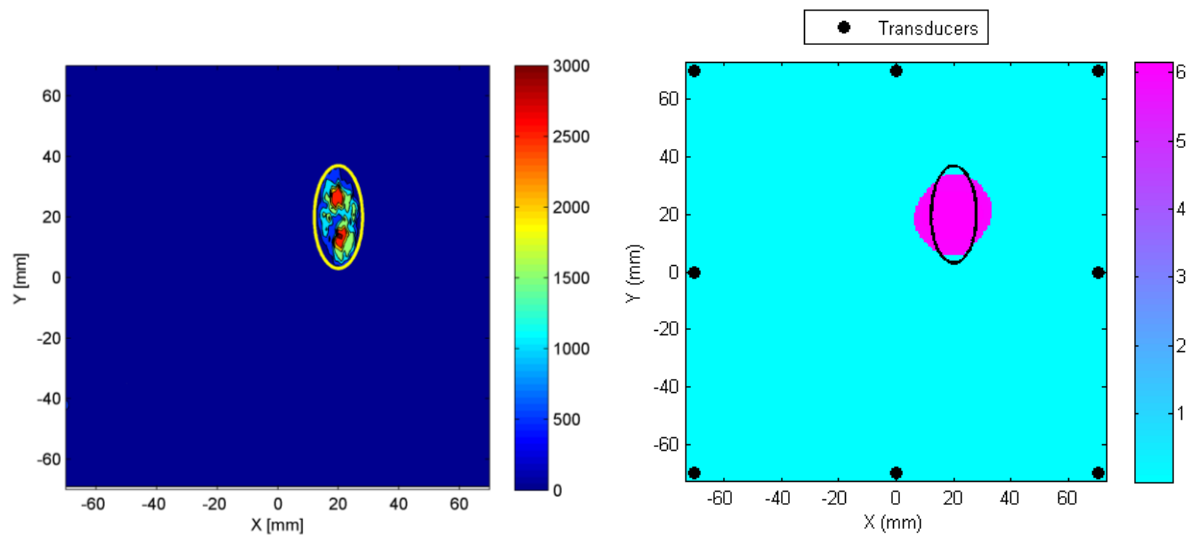


Figure 27: a) C-scan of the plate. b) Damage detection evaluation with 8 transducers.

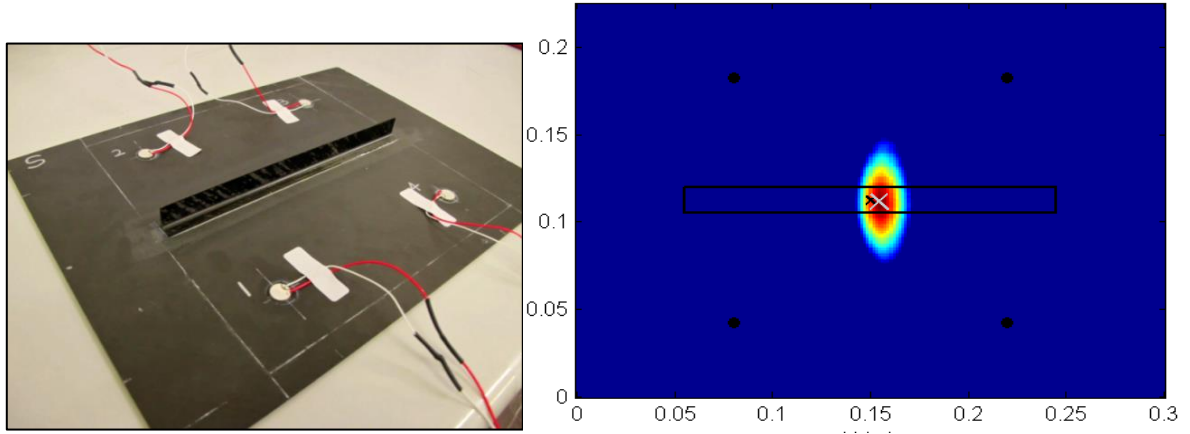


Figure 28: a) Experimental panel. b) debonding detection.



Figure 29: Sub-component specimen with PZTs installed on its inner surface [15].

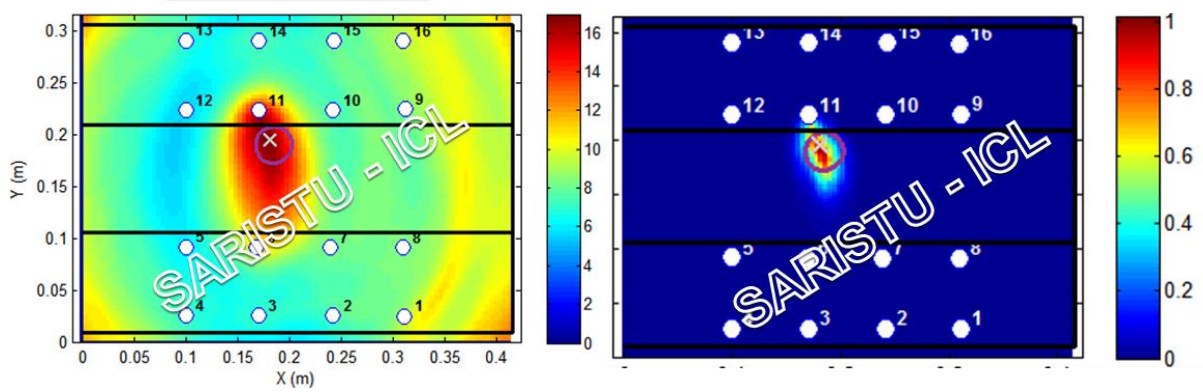
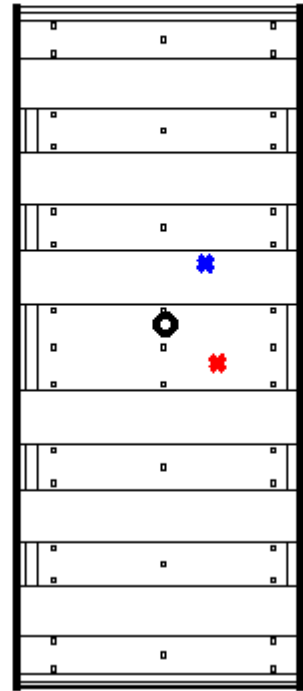
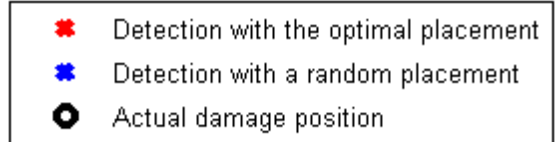
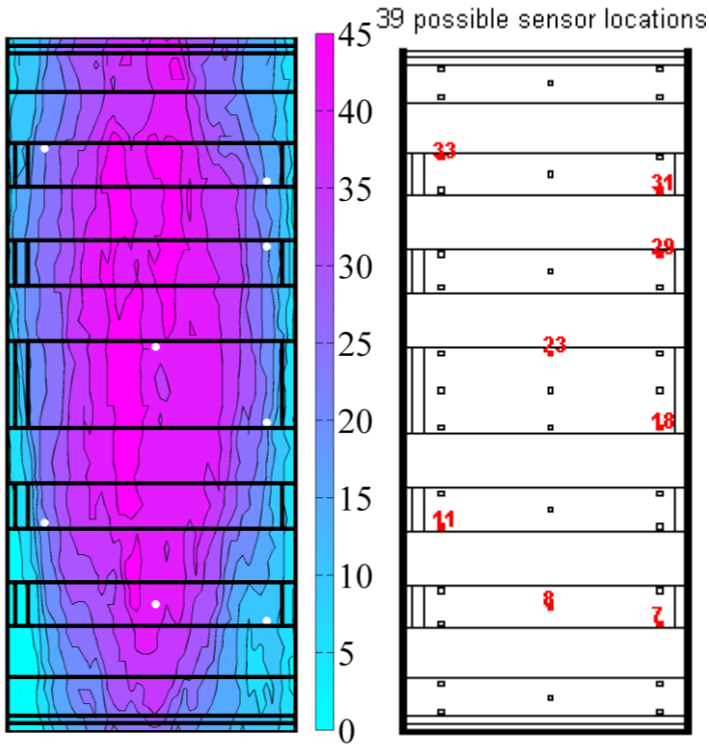


Figure 30: Damage evaluation at sub-component level.



(a) Coverage area of the optimal 8 sensors

(b) Optimal positioning for 8 sensors

(c) Comparison between optimal and random placement for damage detection

Figure 31: Validation of Optimal sensor placement - Active sensing